

# ISVR Technical Memorandum

## SCIENTIFIC PUBLICATIONS BY THE ISVR

*Technical Reports* are published to promote timely dissemination of research results by ISVR personnel. This medium permits more detailed presentation than is usually acceptable for scientific journals. Responsibility for both the content and any opinions expressed rests entirely with the author(s).

*Technical Memoranda* are produced to enable the early or preliminary release of information by ISVR personnel where such release is deemed to be appropriate. Information contained in these memoranda may be incomplete, or form part of a continuing programme; this should be borne in mind when using or quoting from these documents.

*Contract Reports* are produced to record the results of scientific work carried out for sponsors, under contract. The ISVR treats these reports as confidential to sponsors and does not make them available for general circulation. Individual sponsors may, however, authorize subsequent release of the material.

### COPYRIGHT NOTICE

(c) ISVR University of Southampton All rights reserved.

ISVR authorises you to view and download the Materials at this Web site ("Site") only for your personal, non-commercial use. This authorization is not a transfer of title in the Materials and copies of the Materials and is subject to the following restrictions: 1) you must retain, on all copies of the Materials downloaded, all copyright and other proprietary notices contained in the Materials; 2) you may not modify the Materials in any way or reproduce or publicly display, perform, or distribute or otherwise use them for any public or commercial purpose; and 3) you must not transfer the Materials to any other person unless you give them notice of, and they agree to accept, the obligations arising under these terms and conditions of use. You agree to abide by all additional restrictions displayed on the Site as it may be updated from time to time. This Site, including all Materials, is protected by worldwide copyright laws and treaty provisions. You agree to comply with all copyright laws worldwide in your use of this Site and to prevent any unauthorised copying of the Materials.

**A Study of the Performance of a Feedback Active Isolation System  
with Multiple Inertial Actuators**

**R. Paurobally and S. J. Elliott**

**ISVR Technical Memorandum No. 999**

**June 2013**

UNIVERSITY OF SOUTHAMPTON  
INSTITUTE OF SOUND AND VIBRATION RESEARCH  
SIGNAL PROCESSING AND CONTROL GROUP

**A Study of the Performance of a Feedback Active Isolation System with Multiple  
Inertial Actuators**

by

**R. Paurobally, The University of Western Australia  
S. J. Elliott, Institute of Sound and Vibration Research**

ISVR Technical Memorandum No. 999

June 2013

Authorised for issue by  
Professor P. R. White  
Group Chairman

## **Acknowledgement**

The first author would like to thank Professor S. J. Elliott, for the opportunity to visit and work collaboratively with himself at the ISVR. The work presented in this memorandum is supported by the University of Western Australia as part of the first author's study leave.

## CONTENTS

|  | Page |
|--|------|
| 1. Introduction .....  | 1    |
| 2. Review of single-channel case .....                                 | 2    |
| 3. Frequency response of system with multiple inertial actuators ..... | 6    |
| 4. Study of the control of the first mode of a plate .....             | 12   |
| 4.1 Open-loop frequency response of simplified plate model ...         | 12   |
| 4.2 Analysis of control performance of simplified plate model...       | 19   |
| 5. Approximate expression for maximum feedback gain .....              | 20   |
| 6. Performance of control system .....                                 | 27   |
| 7. Summary .....   | 28   |
| 8. References .....  | 30   |

## LIST OF FIGURES

|  | Page |
|--|------|
| 2.1 Schematic of active vibration isolation using an inertial actuator .....   | 2    |
| 2.2 Magnitude and phase of the simulated frequency response of the system with a single inertial actuator .....                        | 4    |
| 2.3 Nyquist plot of the simulated frequency response of the system with a single inertial actuator .....                               | 5    |
| 2.4 Block diagram of a negative feedback control system .....  | 5    |
| 3.1(a) Schematic of active vibration isolation using two inertial actuators .....  | 7    |
| 3.1(b) Free-body diagrams of masses .....  | 7    |
| 4.1(a) Schematic of simplified active vibration isolation of first plate mode using two inertial actuators. ....                       | 12   |
| 4.1(b) Free-body diagrams of individual masses.....  | 12   |
| 4.2 Magnitude and phase of the simulated frequency response of the system when one inertial actuator is used .....                     | 15   |
| 4.3 Nyquist plot of the simulated frequency response of the system when one inertial actuator is used .....                            | 15   |
| 4.4 Magnitude and phase of the simulated frequency response of the system when five identical inertial actuators are used .....        | 16   |
| 4.5 Nyquist plot of the simulated frequency response of the system when five identical inertial actuators are used .....               | 16   |
| 4.6 Magnitude and phase of the simulated frequency response of the system when ten identical inertial actuators are use .....          | 17   |
| 4.7 Nyquist plot of the simulated frequency response of the system when ten identical inertial actuators are use .....                 | 17   |
| 4.8 Magnitude and phase of the simulated frequency response of the system when twenty-five identical inertial actuators are used ..... | 18   |
| 4.9 Nyquist plot of the simulated frequency response of the system when twenty-five identical inertial actuators are used .....        | 18   |

|     |  |    |
|-----|--|----|
| 5.1 | Maximum attenuation from Nyquist simulations due to control only as a function of the number of actuators for 6 dB gain margin.....  | 22 |
| 5.2 | Equivalent representation of the system with multiple actuators for $\omega_a \square \omega_m$ .....  | 23 |
| 5.3 | Predicted variation of resonance frequency and damping ratio of the equivalent plate system from Eqs. (41) and (42).....   | 24 |
| 5.4 | Comparison of simulated (from Nyquist plots) and predicted gains from Eq.(44) and Eq.(49) for 6 dB gain margin.....  | 25 |
| 5.5 | Vibration attenuation for 6 dB gain margin using the equivalent plate analysis of Fig. 5.2. The solid line shows the attenuation achieved in simulations using the Nyquist plots as shown in Fig. 5.1..... | 26 |
| 5.6 | Change in the total kinetic energy of the first plate mode due to passive control, active control and combined passive and active control.....   | 28 |



## 1. INTRODUCTION

This report describes the performance of a feedback active isolation system using multiple inertial actuators based on initial studies by [1] and [4]. In particular, the effect of adding more independent feedback control channels on the stability and active vibration reduction of a single-degree of freedom system is studied. In the first instance, the single-channel problem considered consists of the active isolation of some sensitive equipment from a vibrating base structure through a compliant mount attached between them. The results and limiting factors of using an inertial actuator are clearly introduced and compared to the literature.

In the second instance, the single-channel active isolation system is extended to a two-channel feedback active control system, using two independent inertial actuators. The purpose here is to study the effect of adding more inertial actuators on the stability and performance of the isolation system. In order to achieve this aim the equation representing the system open-loop response of the two-channel system is derived. The effect of coupling of the actuators to the equipment is also demonstrated. The results for the two-channel feedback isolation problem using multiple inertial actuators are then generalized for the multi-channel case.

After the general theory is developed, a simple application to the control of the first vibration mode of a finite plate is presented. An approximate expression for the maximum gain for stable closed-loop operation is derived as well as the expected theoretical vibration attenuation. It is shown that the feedback gain can be accurately predicted for the assumption of a decoupled actuators-plate system as well as the passive reduction in total kinetic energy of the plate. The study shows that increasing the number of actuators increases passive attenuation. However, the reduction due to control alone decreases as the number of control channels increases. The combined passive and active control performance is shown to increase with an increase in inertial control actuators.

## 2. REVIEW OF SINGLE-CHANNEL CASE

In this section a brief review of the main results for the single-channel feedback active isolation problem using an inertial actuator is summarised. The frequency response of a typical system and its Nyquist plot are presented in an example as described in [1]. The approximate maximum gain for closed-loop stability and resulting vibration attenuation are also given.

Figure 2.1 shows the block diagram of the system considered with a single inertial actuator. An inertial actuator is attached to the equipment and generates a secondary force acting on the latter. In Fig. 2.1, the base is assumed flexible and with uncoupled

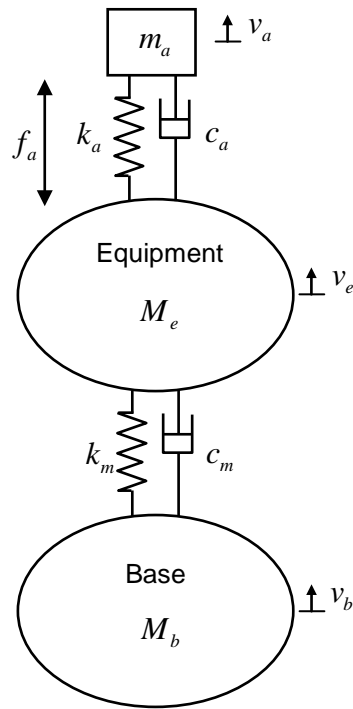


Figure 2.1 Schematic of active vibration isolation using an inertial actuator.

mobility  $M_b$ , the mechanical driving point mobility of the equipment is  $M_e$  and the mount is assumed massless but with a finite mechanical impedance  $Z_m$ . For this system it can be shown that the velocity  $v_e$  of the equipment per unit actuator force  $f_a$  [1] which is proportional to the plant response is given by [2]

$$\frac{v_e}{f_a} = T_a M_{cc} \quad (1)$$

where  $T_a$  is the blocked response of the actuator and  $M_{cc}$  is the input mobility of the coupled system including the passive mount with the inertial actuator attached to it. These are given by the equations [1]

$$T_a = \frac{j\omega m_a}{Z_a + j\omega m_a} \quad (2)$$

$$M_{cc} = \frac{M_{ee}}{1 + Z_{aa} M_{ee}} \quad (3)$$

$$Z_{aa} = \frac{j\omega m_a Z_a}{Z_a + j\omega m_a} \quad (4)$$

where  $m_a$  is the inertial mass,  $Z_a$  the impedance of the actuator suspension given by

$$Z_a = c_a + \frac{k_a}{j\omega} \quad (5)$$

and  $c_a$  and  $k_a$  are the damping constant and stiffness of the actuator suspension respectively.  $\omega$  is the angular frequency.  $M_{ee}$  is the input mobility of the equipment when it is coupled to the mount and base structure and is given by [1]

$$M_{ee} = \frac{M_e (1 + M_b Z_m)}{1 + (M_e + M_b) Z_m} \quad (6)$$

It has been shown previously [1] that because the actuator response is not free of phase shift, the feedback control system can become unstable. To maximize the feedback gain  $g$ , the actuator natural frequency must be designed as low as possible compared with the coupled equipment/mount natural frequency. Consider an example as described in [1] in which the equipment is modeled as a 1.08 kg mass, the mount as a stiffness of 40,000 N/m and a damping of 18 Ns/m. Also let the inertial mass be 0.91 kg and the actuator of stiffness 3,900 N/m and damping 5.8 Ns/m. The simulated frequency response  $G(j\omega)$  of this single inertial actuator system as given

by Eq. (1) is shown in Fig. 2.2. Here the impedance of the mount is assumed to be a pure stiffness  $k_m$ , the mobility of the base as that of a stiffness  $k_b$ , and the mobility of the equipment as a pure mass. It is clear that for a negative feedback control system the critical phase shift of  $\pm 180^\circ$  occurs at the phase crossover frequency which is around the resonance frequency of the actuator. The maximum feedback gain that can be used before instability is thus determined by the magnitude of the frequency response shown in Fig. 2.2 at the phase crossover frequency of about 9 Hz. A Nyquist plot of the simulated plant response is also depicted in Fig. 2.3. The smaller loop on the left with negative real part is due to the actuator resonance which is not well damped. If the gain of the feedback control system is increased, this loop will expand proportionally and the closed-loop system will become unstable when the  $(-1,0)$  point is crossed [3].

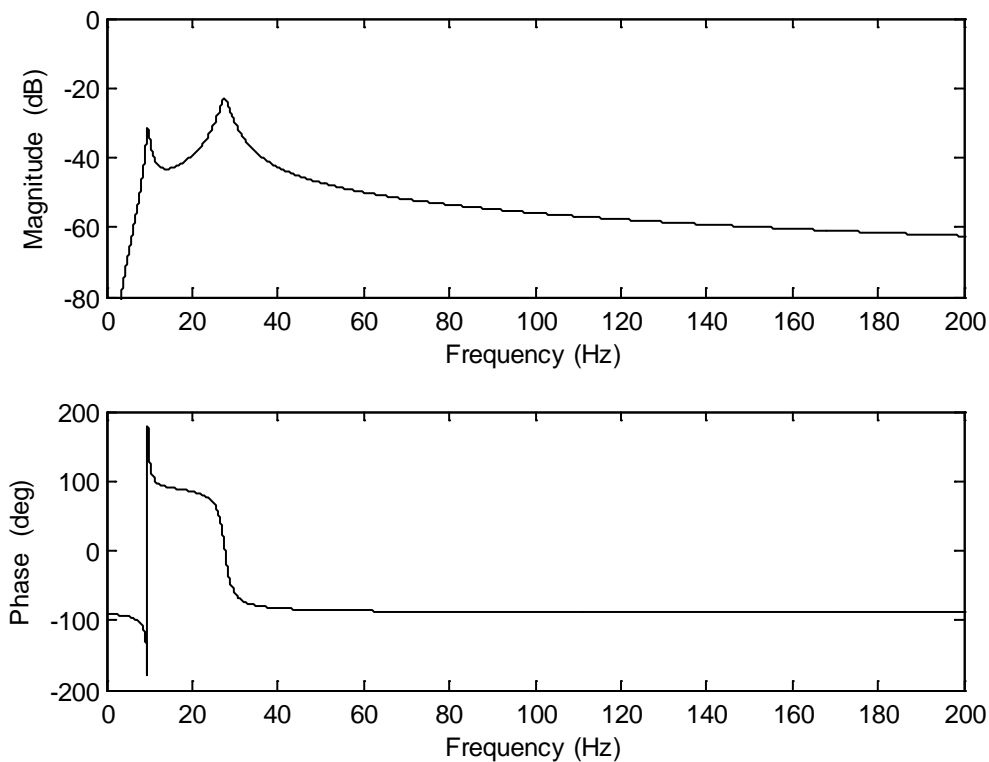


Figure 2.2 Magnitude and phase of the simulated open-loop frequency response of the system with a single inertial actuator.

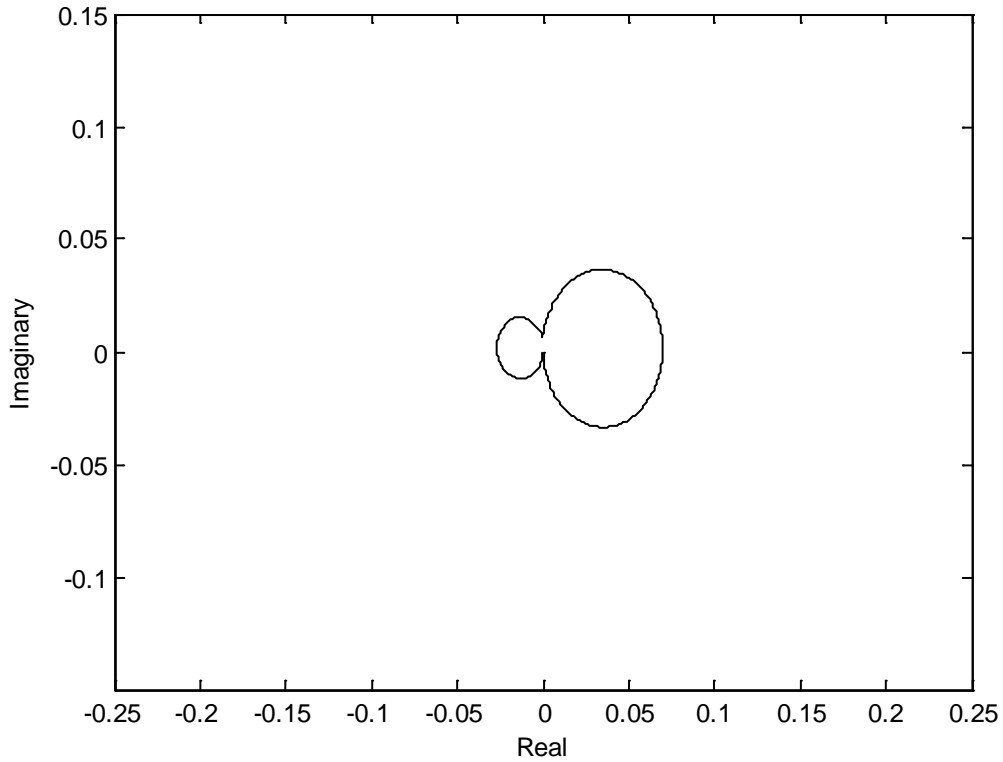


Figure 2.3 Nyquist plot of the simulated open-loop frequency response of the system with a single inertial actuator.

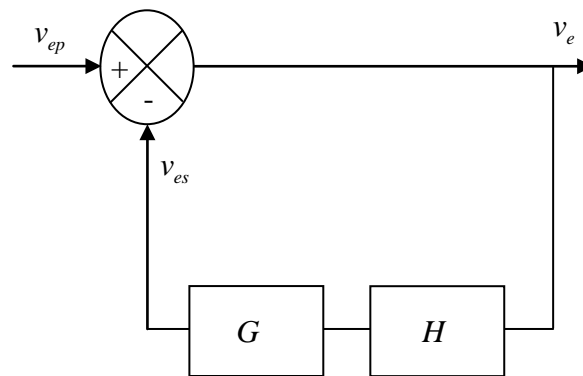


Figure 2.4 Block diagram of a negative feedback control system.

If the feedback control system is connected in negative feedback configuration as shown in Fig. 2.4, where  $H$  represents the controller, then the closed-loop response is given by

$$\frac{v_e}{v_{ep}}(j\omega) = \frac{1}{1 + G(j\omega)H(j\omega)} \quad (7)$$

where  $v_{ep}$  is the primary disturbance velocity of the equipment before active control. This equation represents the vibration reduction due to control only excluding the

passive attenuation effects of the actuators. Assuming that a simple-gain controller is employed, an approximate expression for the maximum gain that can be used to guarantee stability can be obtained. This also leads to the approximate maximum vibration attenuation that can be achieved by feedback control using the inertial actuator. If the natural frequency of the actuator,  $\omega_a$ , is much less than that of the first natural frequency  $\omega_m$ , of the mounted equipment, then the maximum gain is given by [1]

$$g_{\max} = \frac{2\xi_a m_e \omega_m^2}{\omega_a} = \frac{c_a k_m}{k_a} \quad (8)$$

where  $\xi_a$  is the damping ratio of the actuator,  $m_e$  the mass of the equipment and  $k_m$  is the stiffness of the mount. The vibration attenuation corresponding to half the maximum gain given in Eq. (8) can be obtained using Eq. (7) as

$$Attn (dB) = -20 \log_{10} \left( \frac{2\xi_m \omega_a}{2\xi_m \omega_a + \xi_a \omega_m} \right) \quad (9)$$

Equation (9) shows that the attenuation can be made high provided that the natural frequency of the actuator is small compared to the first natural frequency of the equipment and also that the actuator must be well damped compared with this equipment mode. In the next section a general model of the system with multiple inertial actuators is presented in order to obtain the total open-loop frequency response of the system. This will subsequently be used to study the performance of the control of the first mode of a plate of a system.

### 3. FREQUENCY RESPONSE OF SYSTEM WITH MULTIPLE INERTIAL ACTUATORS

In this section the case of using two inertial actuators for feedback active isolation is considered. The equations for the frequency responses of the system are derived to show the effect of adding one more actuator on its closed-loop stability and the vibration attenuation. Figure 3.1(a) shows a schematic of the system studied.

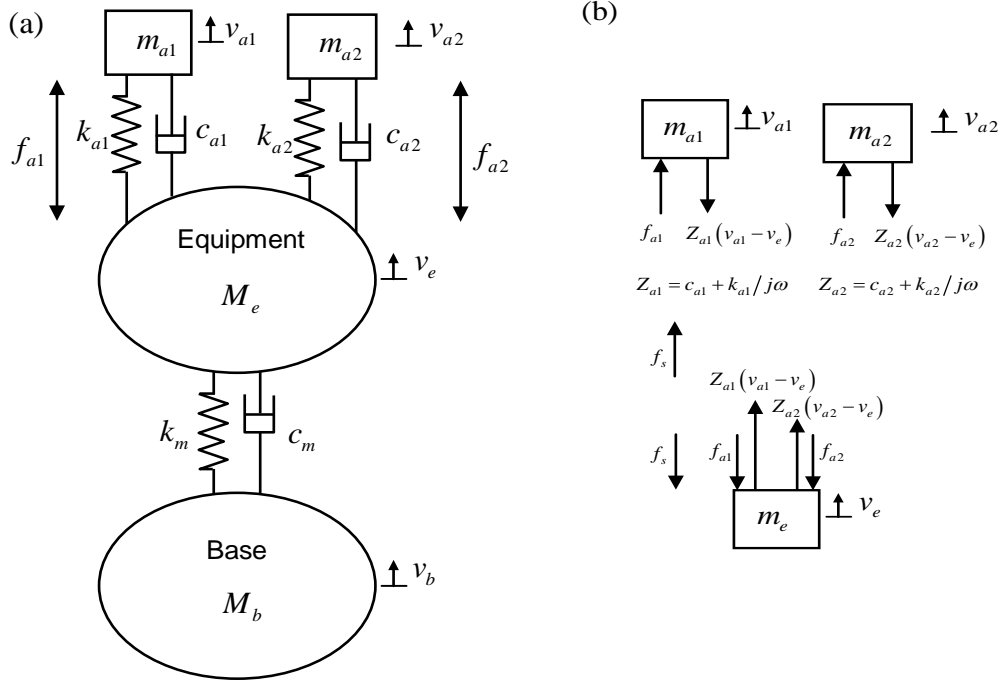


Figure 3.1 (a) Schematic of active vibration isolation using two inertial actuators.  
 (b) Free-body diagrams of masses.

It is possible to represent the system in Fig. 3.1(a) by the free-body diagrams shown in Fig. 3.1(b) in order to derive the equations of motion of each mass. The total secondary force  $f_s$  acting down on the mass  $m_e$  is then given by

$$f_s = [f_{a1} + f_{a2} - Z_{a1}(v_{a1} - v_e) - Z_{a2}(v_{a2} - v_e)] \quad (10)$$

where  $Z_{a1}$  and  $Z_{a2}$  are the impedances of the actuators. The equations of motion for each inertial mass can also be written as:

Mass  $m_{a1}$ :

$$f_{a1} - Z_{a1}(v_{a1} - v_e) = j\omega m_{a1} v_{a1} \quad (11)$$

Mass  $m_{a2}$ :

$$f_{a2} - Z_{a2}(v_{a2} - v_e) = j\omega m_{a2} v_{a2} \quad (12)$$

Substitution of Eqs. (11) and (12) into (10) results in the following equation.

$$f_s = \left[ f_{a1} \left( \frac{j\omega m_{a1}}{Z_{a1} + j\omega m_{a1}} \right) + f_{a2} \left( \frac{j\omega m_{a2}}{Z_{a2} + j\omega m_{a2}} \right) + v_e \left( \frac{j\omega Z_{a1} m_{a1}}{Z_{a1} + j\omega m_{a1}} + \frac{j\omega Z_{a2} m_{a2}}{Z_{a2} + j\omega m_{a2}} \right) \right] \quad (13)$$

It is possible to define the mechanical input impedance of  $m_{a1}$  and  $m_{a2}$  respectively by the equations

$$Z_{aa1} = \frac{j\omega Z_{a1} m_{a1}}{Z_{a1} + j\omega m_{a1}} \quad \text{and} \quad Z_{aa2} = \frac{j\omega Z_{a2} m_{a2}}{Z_{a2} + j\omega m_{a2}} \quad (14)$$

If the equipment is held fixed then  $v_e = 0$  and the blocked response of the system when both actuators are in operation is given by

$$f_{sb} = \left[ f_{a1} \left( \frac{j\omega m_{a1}}{Z_{a1} + j\omega m_{a1}} \right) + f_{a2} \left( \frac{j\omega m_{a2}}{Z_{a2} + j\omega m_{a2}} \right) \right] \quad (15)$$

Also if only actuator 1 was generating the force on the equipment at any time, then the blocked response of actuator 1 can be defined as

$$\frac{f_{sb}}{f_{a1}} = \frac{j\omega m_{a1}}{Z_{a1} + j\omega m_{a1}} = T_{a1} \quad (16)$$

Similarly the blocked response for actuator 2 when it generates the only force is defined as

$$\frac{f_{sb}}{f_{a2}} = \frac{j\omega m_{a2}}{Z_{a2} + j\omega m_{a2}} = T_{a2} \quad (17)$$

The secondary force acting on the equipment as given by Eq. (13) can be simplified using the above equations as

$$f_s = [f_{a1} T_{a1} + f_{a2} T_{a2} + Z_{aa} v_e] \quad (18)$$

where  $Z_{aa}$  is the total mechanical input impedance of the inertial actuators as seen at the connection point of the equipment. It is given by

$$Z_{aa} = Z_{aa1} + Z_{aa2} \quad (19)$$



If the equipment is assumed rigid and both actuators are driven simultaneously with the same input to give a total force  $f_{aT} = f_{a1} + f_{a2}$  and velocity  $v_e$ , then it is possible to define the frequency responses  $G_1$  and  $G_2$  of the system with respect to each actuator as

$$G_1 = \frac{v_e}{f_{a1}} \quad (20)$$

$$G_2 = \frac{v_e}{f_{a2}} \quad (21)$$

The velocity  $v_e$  will be generated by  $f_s$  via the input mobility  $M_{ee}$  as defined in Eq. (6) of the equipment on the passive mount. That is,

$$v_e = M_{ee} f_s \quad (22)$$

The response of the system can be obtained from Eqs. (18) to (22) as

$$v_e [1 + M_{ee} Z_{aa}] = M_{ee} [f_{a1} T_{a1} + f_{a2} T_{a2}] \quad (23)$$

It is possible to derive the frequency responses defined in Eqs. (20) and (21) for the two-channel active isolation system by using Eq. (23). They are given by

$$G_1 = \frac{v_e}{f_{a1}} = \frac{M_{ee}}{[1 + M_{ee} Z_{aa}]} \left[ T_{a1} + \frac{f_{a2}}{f_{a1}} T_{a2} \right] \quad (24)$$

$$G_2 = \frac{v_e}{f_{a2}} = \frac{M_{ee}}{[1 + M_{ee} Z_{aa}]} \left[ \frac{f_{a1}}{f_{a2}} T_{a1} + T_{a2} \right] \quad (25)$$

Assuming that the actuators generate identical forces such that  $f_{a1} = f_{a2} = f_a$  and also  $T_{a1} = T_{a2} = T_a$ , then  $G_1 = G_2 = G$ , given by

$$G = \frac{v_e}{f_a} = 2M_{cc2} T_a \quad (26)$$

$$M_{cc2} = \frac{M_{ee}}{[1 + M_{ee} Z_{aa}]} = \frac{M_{ee}}{[1 + M_{ee} (Z_{aa1} + Z_{aa2})]} \quad (27)$$

$M_{cc2}$  is an equivalent input mobility of the coupled system including the passive mount with the two inertial actuators attached to it. Therefore compared to the single-channel case (see Eq. (1)) the frequency response of the actuators in the two-channel

system is modified by a factor of 2 as well as by a change in the total mechanical input impedance  $Z_{aa}$ . As a result, the maximum controller gain for each channel will need to be reduced to guarantee stability. The effect of adding more than 2 actuators to the system can also be studied by extending the study above for the two-channel case as shown next.

It is interesting to point out that if the actuators can be assumed decoupled with the equipment such that  $M_{ee}Z_{aa1} \ll 1$  and  $M_{ee}Z_{aa2} \ll 1$  then Eq. (26) reduces to

$$\frac{v_e}{f_a} = 2M_{ee}T_a \quad (28)$$

If a single actuator was employed and the actuator was decoupled with the equipment, the response [1] can be obtained from Eq. (1) as

$$\frac{v_e}{f_a} = M_{ee}T_a \quad (29)$$

Hence, with two identical actuators the magnitude of the frequency response is simply doubled since  $M_{ee}$  and  $T_a$  are constants independent of the number of actuators used.

When more than two actuators are used, it is possible to generalize the results for the frequency responses of the system per actuator input force. Consider  $n$  actuators mounted on the rigid equipment. Then Eq. (23) can be extended to

$$v_e \left[ 1 + M_{ee} (Z_{aa1} + \dots + Z_{aan}) \right] = M_{ee} \left[ f_{a1}T_{a1} + \dots + f_{an}T_{an} \right] \quad (30)$$

The frequency response of each actuator  $j$  can then be obtained from the equation

$$\frac{v_e}{f_{aj}} = \left[ \frac{M_{ee}}{1 + M_{ee} (Z_{aa1} + Z_{aa2} + \dots + Z_{aan})} \right] \left[ \sum_{i=1}^n \frac{f_{ai}T_{ai}}{f_{aj}} \right] = M_{ccn} \left[ \sum_{i=1}^n \frac{f_{ai}T_{ai}}{f_{aj}} \right] \quad (31)$$

where the total input mobility of the coupled system  $M_{ccn}$  is now given by

$$M_{ccn} = \frac{M_{ee}}{\left[ 1 + M_{ee} (Z_{aa1} + Z_{aa2} + \dots + Z_{aan}) \right]} \quad (32)$$

The frequency response given in Eq. (31) can further be simplified to

$$\frac{v_e}{f_{aj}} = M_{ccn} \left[ \sum_{i=1}^n r_{ij} T_{ai} \right], \quad r_{ij} = \frac{f_{ai}}{f_{aj}} \quad (33)$$

For the case of  $n$  ideal actuators,  $r_{ij} = 1$  and assuming  $T_{ai} = T_a$  the frequency response for each individual actuator is given by

$$\frac{v_e}{f_{aj}} = nM_{ccn}T_a \quad (34)$$

Therefore, for the general case when multiple inertial actuators are used in an active isolation system, the magnitude of the frequency response is increased  $n$  times as well as modified by the total mechanical impedance  $Z_{aa}$  of the actuators.

If the equipment and actuators can be assumed decoupled similar to the case of the single and two-actuator cases earlier, then Eq. (34) can be simplified to

$$\frac{v_e}{f_{aj}} = nM_{ee}T_a \quad (35)$$

Compared to Eq. (29) for the single actuator case, the frequency response magnitude of the decoupled equipment/multiple-actuators case is  $n$  times that of the single-actuator case. It is possible to obtain an expression for the maximum feedback gain of the controller for each channel to ensure closed-loop stability and also an expression for the corresponding vibration reduction. This is the subject of section 5 after an example of the control of the first mode of a plate is presented in section 4. It is shown that under the decoupled assumption, a valid expression for the maximum gain can be derived as well as an expression for the peak vibration attenuation for a varying number of actuators.

#### 4. STUDY OF THE CONTROL OF THE FIRST MODE OF A PLATE

In this section, an example of the use of multiple inertial actuators to control the first mode of a plate [4] using the model described in section 3 is presented. In section 4.1, a simplified model of the open-loop frequency response of the system is presented and the effect of adding more actuators studied. Then in section 4.2, the general equation for the mobility of the plate including any number of inertial actuators with control is derived. This is then used to study the performance of the system with multiple actuators in terms of the change in total kinetic energy of the plate mode.

##### 4.1 Open-loop frequency response of simplified plate model

A simplified model of a plate is shown in Fig. 4.1 with the base assumed rigid, i.e. its mobility  $M_b = 0$ . The mass of the equipment is assumed equivalent to that of the plate considered including the vibration sensor casing, and with finite plate stiffness  $k_m$  and plate damping  $c_m$ . A primary disturbance force  $f_p$  is also shown acting on the plate causing it to vibrate. All other variables remain as defined in section 3.

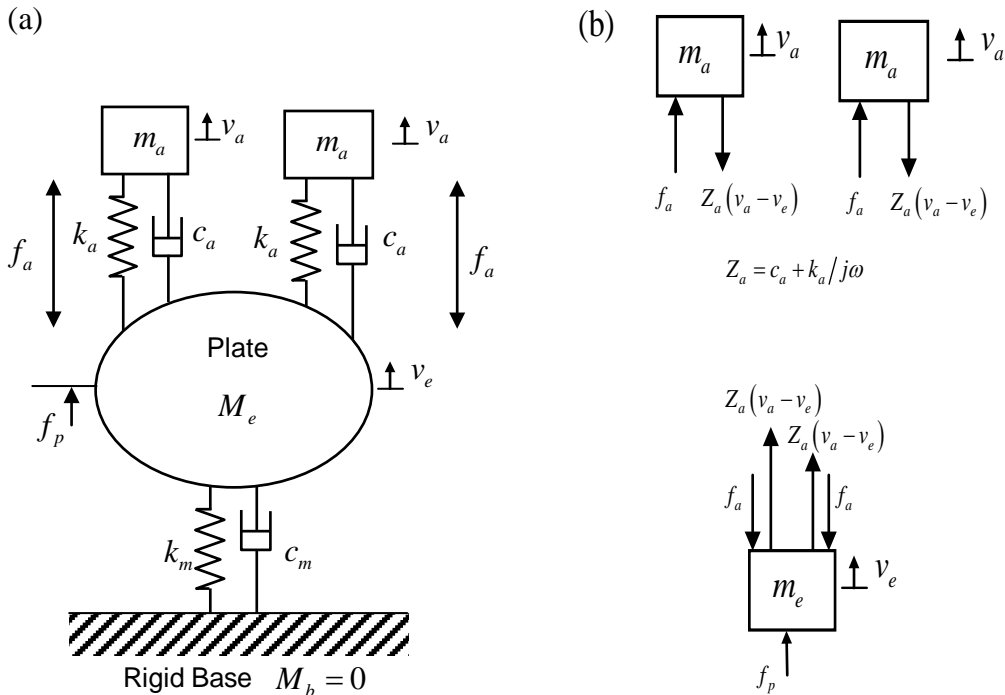


Figure 4.1 (a) Schematic of simplified active vibration isolation of first plate mode using two inertial actuators. (b) Free-body diagrams of individual masses.

For this system, the generalized open-loop frequency response is still given by Eq.(34) but with  $M_{ee}$  given in Eq.(6) modified assuming  $M_b = 0$  to

$$M_{ee} = \frac{M_e}{1 + M_e Z_m} \quad (36)$$

Equation (34) can then still be used to study the open-loop frequency response of a multi-actuator system. Consider an example of a physical system with the parameters given in Table 4.1 [4]. The plate is assume to be a rigid mass  $m_e$  (including sensor casing mass  $m_c$ ) connected to a fixed base with a stiffness  $k_m$  and damping  $c_m$ . The actuators are assumed identical with mass  $m_a$ , stiffness  $k_a$  and damping  $c_a$ . For the purpose of analysis and simulation the force constant of the linear current amplifier is assumed to be equal to 1  $N/A$ .

Table 4.1 Table of physical system parameters.

| Parameter      | Value      |
|----------------|------------|
| $m_e$          | 2.226 kg   |
| $k_m$          | 126897 N/m |
| $c_m$          | 18 Ns/m    |
| $m_c$          | 0.050 kg   |
| $m_a$          | 0.032 kg   |
| $k_a$          | 140 N/m    |
| $c_a$          | 1.39 Ns/m  |
| Force constant | 1 N/A      |

In the absence of the primary disturbance  $f_p$  it is possible to obtain the open-loop frequency response of the system in Fig. 4.1 fitted with 1, 5, 10 and 25 actuators with respect to the input actuator force. The frequency response and Nyquist plots for any

actuator-sensor pair are identical and as depicted in Figs. 4.2 to 4.9 respectively. It is clear that the magnitude of the frequency response changes around the resonances and the loops of the Nyquist plots expand compared to the single channel case in Fig. 4.2. The plots are useful in determining the maximum gain that can be used to optimize the performance of the system while ensuring robust stability of the closed-loop system.

Around the first resonance of about 11 Hz the magnitude increases almost proportionally with the number of actuators. This actuator-related resonance also shifts slightly towards lower frequencies although this is not clearly visible for the well-damped actuator used here. The second resonance around 38 Hz is related to the coupled mounted resonance frequency of the plate. This plate-related resonance shifts slightly to higher frequencies and also becomes a bit more damped such that its peak magnitude changes relatively less. As a result the net effect on the frequency response is such that the right-hand loop in the Nyquist plots tends to expand at a relatively slower rate compared to the left-hand loop. Therefore, in order to keep this system stable the maximum feedback gain of each channel will depend mainly on the magnitude at the first resonance frequency at the phase-crossover frequency. The maximum vibration attenuation however, is limited by the fact that the right-hand loop which is related to the plate first resonance increases at a slower rate than the left-hand loop which is related to the actuator resonance. This effect would have been more prominent if the actuator damping was smaller such that the first resonance frequency was of similar magnitude to the second resonance. The model shows that for good stability it is clearly desirable to keep the actuator damping high.

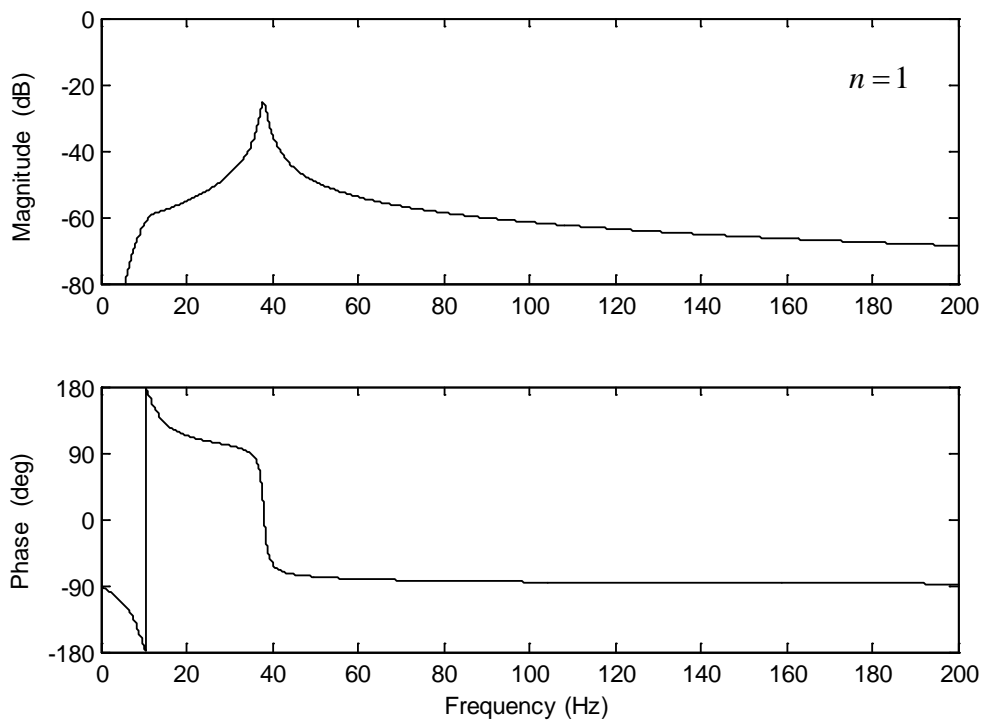


Figure 4.2 Magnitude and phase of the simulated open-loop frequency response of the system when one inertial actuator is used.

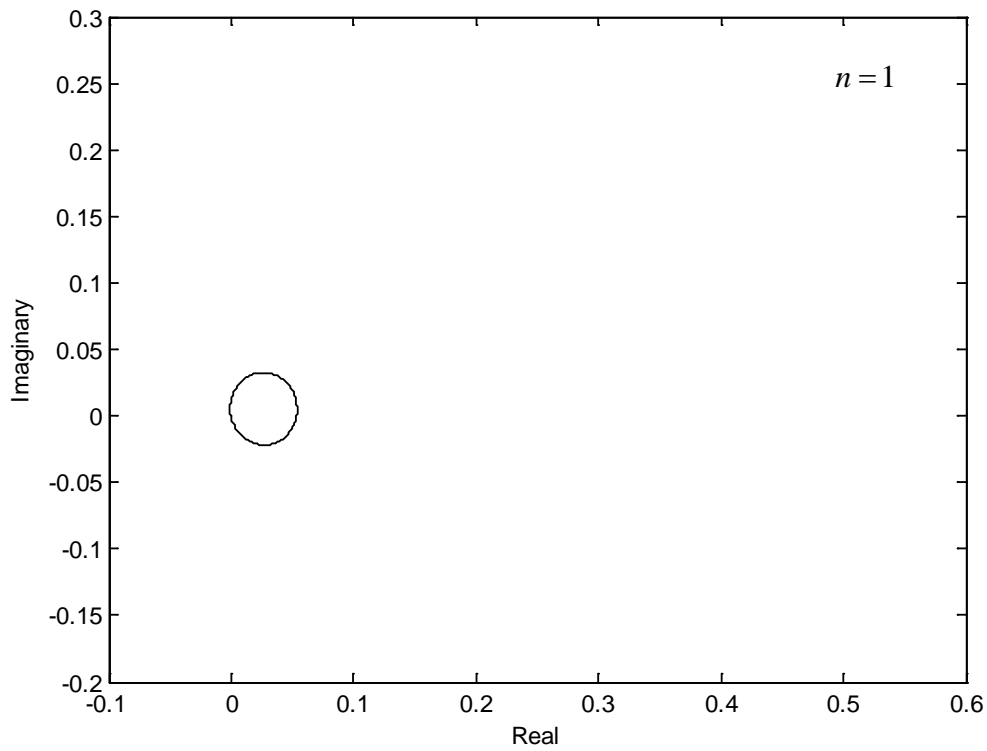


Figure 4.3 Nyquist plot of the simulated open-loop frequency response of the system when one inertial actuator is used.

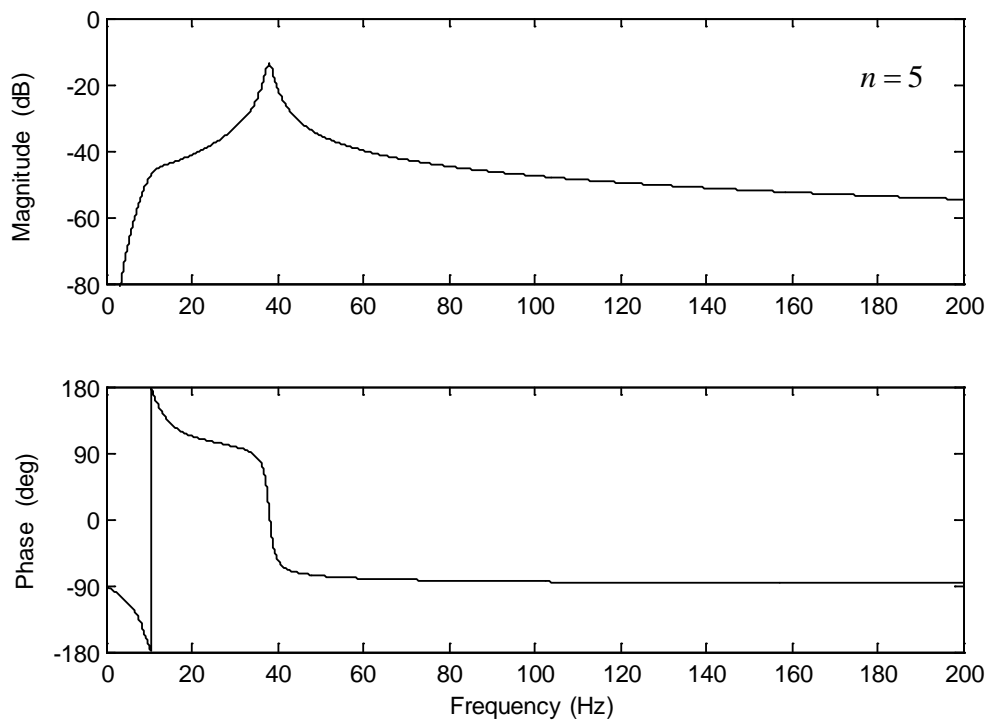


Figure 4.4 Magnitude and phase of the simulated open-loop frequency response of the system when five identical inertial actuators are used.

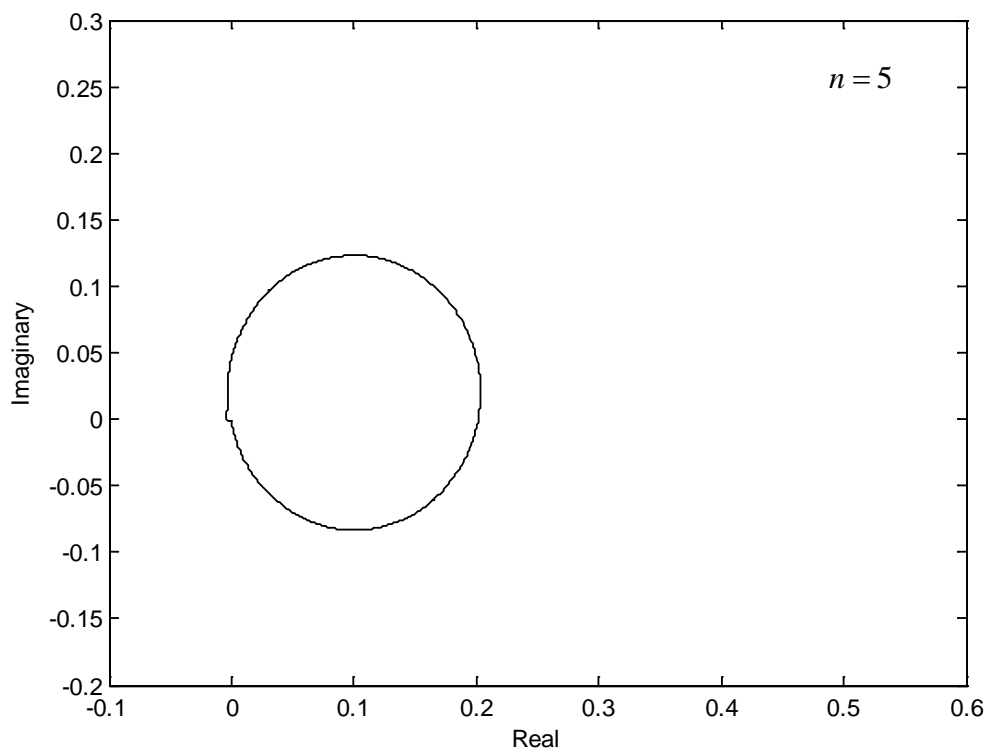


Figure 4.5 Nyquist plot of the simulated open-loop frequency response of the system when five identical inertial actuators are used.



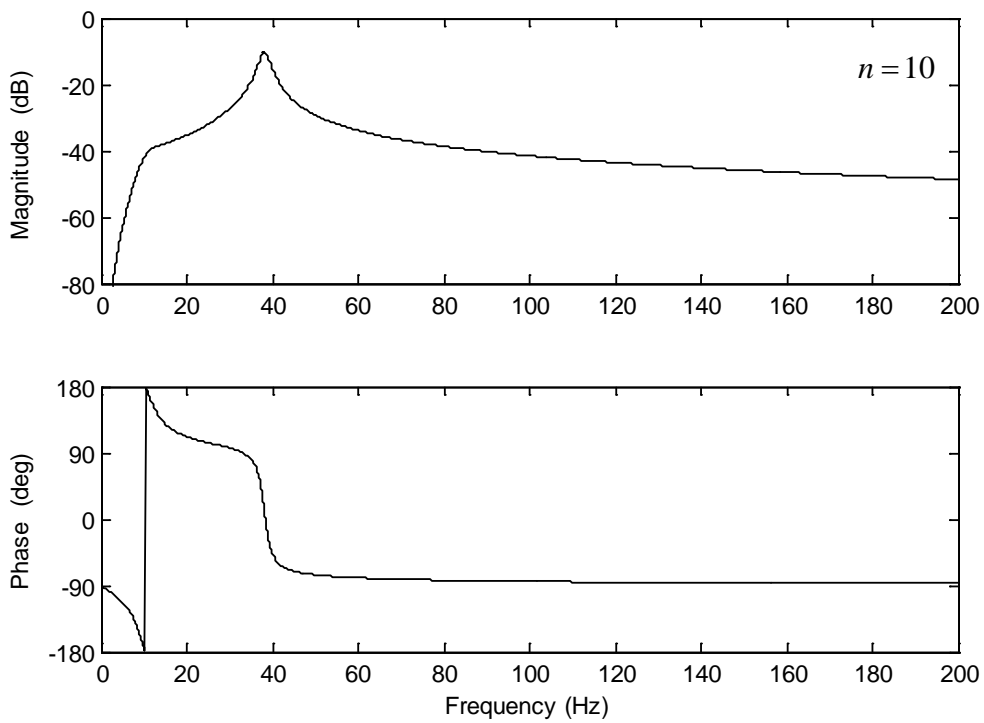


Figure 4.6 Magnitude and phase of the simulated open-loop frequency response of the system when ten identical inertial actuators are used.

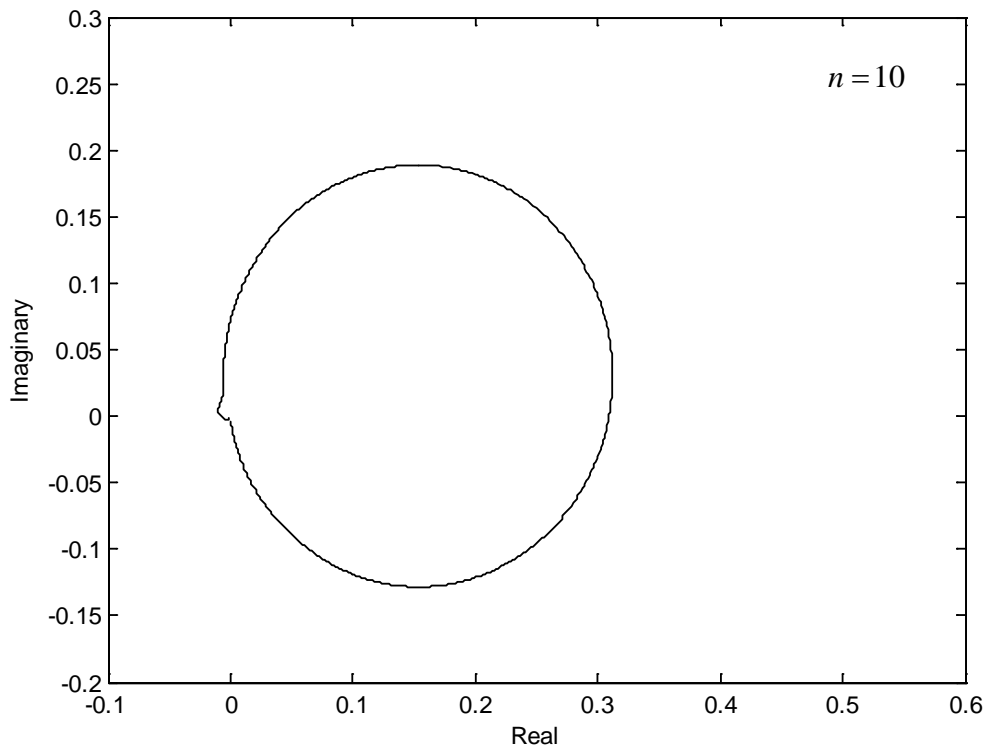


Figure 4.7 Nyquist plot of the simulated open-loop frequency response of the system when ten identical inertial actuators are used.

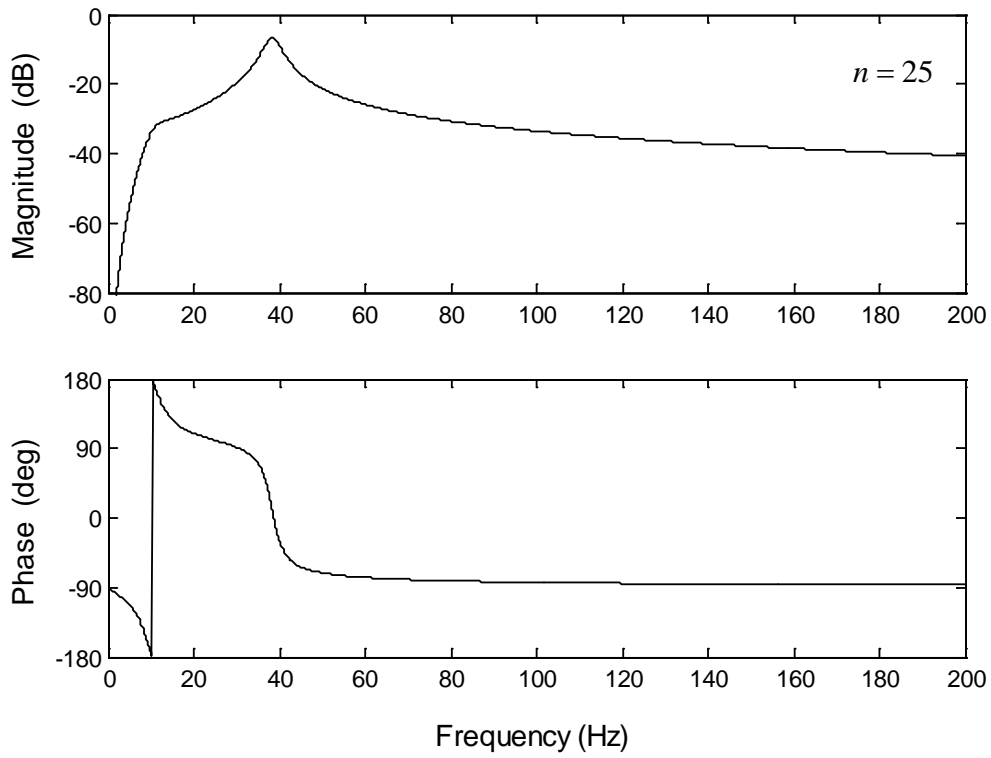


Figure 4.8 Magnitude and phase of the simulated open-loop frequency response of the system when twenty-five identical inertial actuators are used.

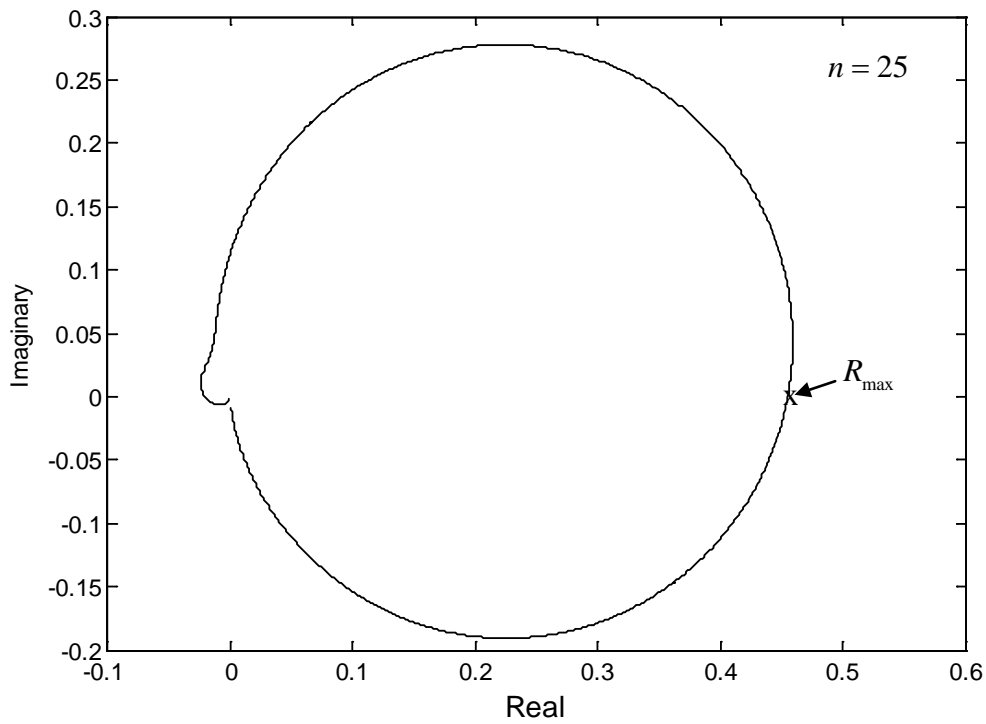


Figure 4.9 Nyquist plot of the simulated frequency response of the system when twenty-five identical inertial actuators are used.

#### 4.2 Analysis of control performance of simplified plate model

The free-body diagrams in Fig. 4.1 (b) can be used to derive an expression for the mobility of the first plate mode including control. The following frequency domain equation can be obtained for each actuator.

$$f_a + Z_a v_e = (Z_a + j\omega m_a) v_a \quad (37)$$

A force balance of the plate mass leads to Eq. (37).

$$f_p - 2f_a + 2Z_a v_a = (2Z_a + Z_m + j\omega m_e) \quad (38)$$

If the sensors are assumed ideal and the amplifiers to drive the actuators have a unit force constant, the control force for a given feedback gain  $g$  is

$$f_a = g v_e \quad (39)$$

Manipulation of the above equations leads to the mobility of the plate for the case of 2 actuators given by

$$\frac{v_e}{f_p} = \frac{1}{[2Z_a + Z_m + j\omega m_e] - 2 \left[ \frac{Z_a (g + Z_a)}{(Z_a + j\omega m_a)} - g \right]} \quad (40)$$

For the case of  $n$  identical inertial actuators the above derivation can be easily extended to get the general equation for the mobility of the plate with control as given in Eq. (41).

$$\frac{v_e}{f_p} = \frac{1}{[nZ_a + Z_m + j\omega m_e] - n \left[ \frac{Z_a (g + Z_a)}{(Z_a + j\omega m_a)} - g \right]} \quad (41)$$

This equation can be used to study the change in the total kinetic energy ( $\frac{1}{2} m_a v_e \cdot v_e^*$ ) of the plate mode per unit primary disturbance for several cases including the effect of control ( $n \geq 1, g \neq 0$ ) and without control but with actuators attached ( $n \geq 1, g = 0$ ). Also, when  $n = 0$ , the kinetic energy of the plate per unit disturbance without any actuators attached can be obtained.

Before the performance of the multiple-actuators control system can be studied for the simplified system, the gain required to guarantee stability and achieve some predefined gain margin must be obtained. An approximate expression for the feedback gain is presented in the next section. The performance of the control system in terms of reduction in total kinetic energy of the plate is then discussed in section 6.

## 5. APPROXIMATE EXPRESSION FOR MAXIMUM FEEDBACK GAIN

It is possible to derive an approximate maximum equal gain for each channel by assuming that the actuators are decoupled to the plate. That is, when the actuator resonance frequency  $\omega_a$  is much less than the mounted resonance frequency  $\omega_m$  of the first plate mode [1]. The frequency response plots shown in section 4.1 show that the stability of the system is dependent upon the actuator resonance frequency. The total open-loop response of the control system for  $n$  actuators, assuming a decoupled system, is then given by the equation

$$GH = nM_{ee}T_a g \quad (42)$$

where  $H = g$  is the feedback controller gain for each channel. Following a similar approach to that described in [1] it can be shown that for the case of multiple actuators, the corresponding maximum gain can be derived as

$$g_{\max} = \frac{2\xi_a m_e \omega_m^2}{n\omega_a} = \frac{c_a k_m}{nk_a} \quad (43)$$

Hence compared to the single-channel case, the maximum gain  $g_{\max}$  is now  $n$  times less than that given in Eq. (8). This tends to agree with the fact that the magnitude of the frequency response at the first resonance has increased by a factor of  $n$ . The approximate maximum vibration attenuation due to the effect of control alone for half the gain given in Eq. (43), that is when

$$g_{\delta dB} = \frac{\xi_a m_e \omega_m^2}{n\omega_a} = \frac{c_a k_m}{2nk_a} \quad (44)$$

can also be obtained from Eq. (7) at  $\omega = \omega_n$ . This is given by

$$Attn (dB) = -20 \log_{10} \left( \frac{2\xi_m \omega_a}{2\xi_m \omega_a + \xi_a \omega_m} \right) \quad (45)$$

It is exactly the same as the expression given in Eq. (9) for the single channel case. Hence for the case studied here and the decoupled assumption made, the expression given in Eq. (45) suggests that the performance of the system stays the same irrespective of the number of independent control channels used. Clearly this simple expression breaks down for the example given here since the frequency responses and Nyquist plots show that the maximum attenuation is not constant. In fact, it tends to decrease with an increasing number of actuators. The assumption that the actuators do not affect the response of the structure does not hold for the system considered here and the expression for maximum vibration reduction with multiple actuators as given in Eq. (45) needs to be modified.

The peak vibration attenuation can be plotted as a function of the number of actuators used for a given gain margin of say 6 dB. For this case the negative real intercept on the Nyquist plots is fixed at 0.5 by adjusting the feedback gain of each channel. This can easily be done in simulation and the peak attenuation then obtained using Eq. (7). An approximate expression for the peak attenuation at the second resonance frequency can be calculated using the equation

$$Attn (dB) = -20 \log_{10} \left( \frac{1}{1 + R_{\max}} \right) \quad (46)$$

where  $R_{\max}$  is the real intercept of the optimised right-hand loop of the Nyquist plot as depicted in Fig. 4.9. A plot of the simulated peak vibration attenuation is given in Fig. 5.1 for the number of actuators varying from 1 to 25.

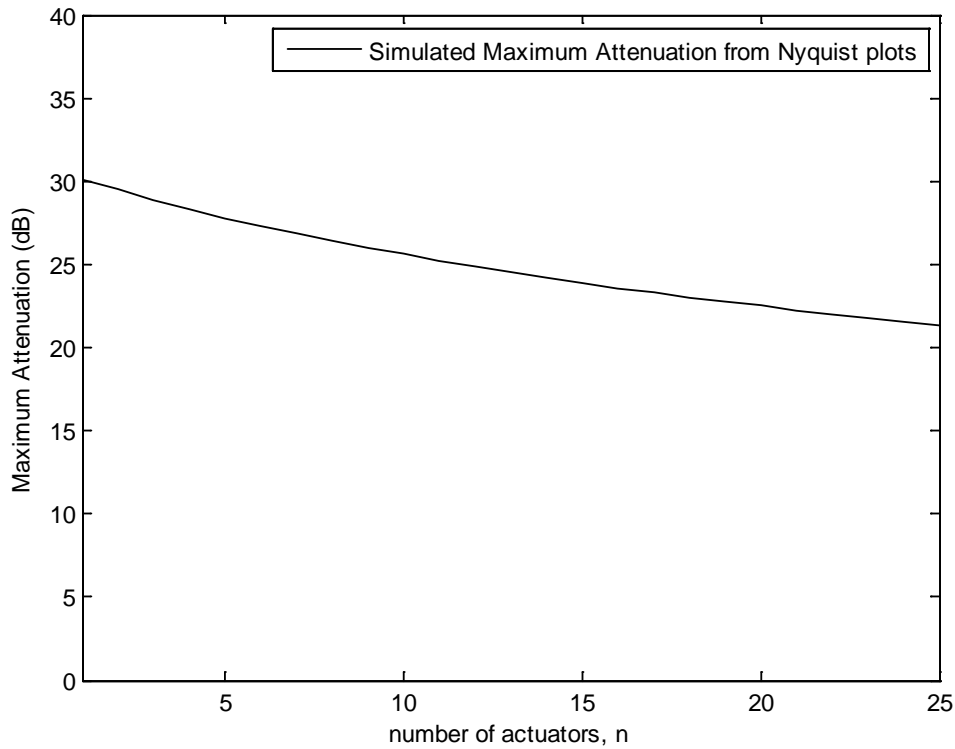


Fig. 5.1 Maximum attenuation from Nyquist simulations due to control only as a function of the number of actuators for 6 dB gain margin.

As the number of actuators increases, the peak attenuation that can be achieved for a gain margin of 6 dB decreases. This result can be explained from the fact that the addition of more actuators, changes the frequency response of the system by modifying the coupled mobility of the plate-actuators system as discussed previously. The frequency response and Nyquist plots shown in Figs. 4.2 to 4.9 also confirm the result of Fig. 5.1 since the magnitude of the second resonance becomes more damped.

In order to obtain a more realistic approximate expression for the vibration attenuation of the multiple-actuator system it is possible to represent the decoupled actuators-plate system for  $\omega_a \ll \omega_m$ , as depicted in Fig. 5.2. During operation at  $\omega = \omega_m$  the actuators are assumed to be well above their natural frequency  $\omega_a$ , so that they are stiffness and damping controlled, and the actuator masses can be assumed to be at rest. The actuators stiffness and damping thus appear connected to an inertial ground shown on the left hand side of Fig. 5.2 and incorporated into the plate stiffness and damping on the right hand side. The plate mass with actuators attached thus behaves like an equivalent system with the plate stiffness and damping altered by the actuators stiffness and damping.

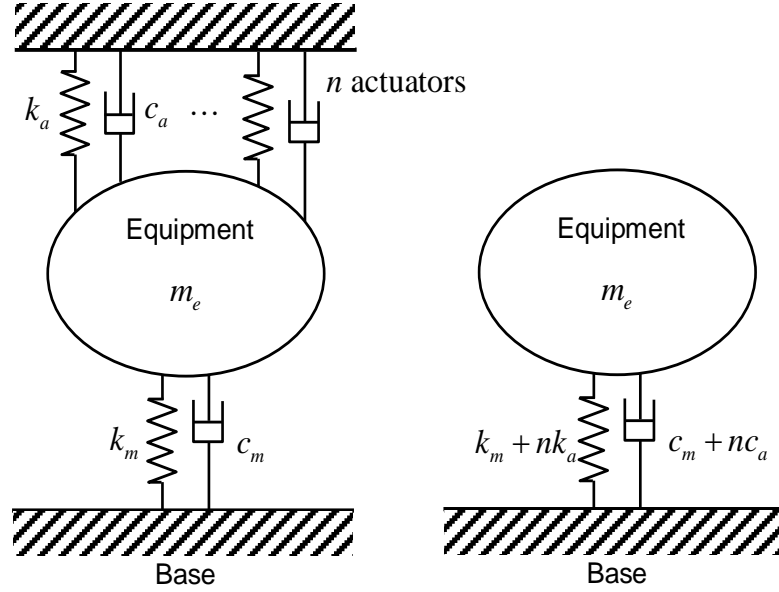


Fig. 5.2 Equivalent representation of the system with multiple actuators for  $\omega_a \ll \omega_m$ .

For the equivalent system, the mount stiffness and damping are modified by the addition of  $n$  times the stiffness and damping of each actuator. The resonance frequency and damping ratio of this equivalent system are given by

$$\omega_m = \sqrt{\frac{k_m + nk_a}{m_e}} \quad (47)$$

$$\xi_m = \frac{c_m + nc_a}{2\sqrt{m_e(k_m + nk_a)}} \quad (48)$$

These equations represent the change in the stiffness and damping of the plate due to the addition of the undriven actuators. In particular Eq.(48) gives an indication of the ‘passive’ attenuation effect before control is even applied. The approximate peak vibration reduction can then be calculated from Eq. (45) with the modified parameters given in Eqs. (47) and (48). The resonance frequency and damping ratio given by these equations can be plotted as a function of the number of actuators for the plate example considered earlier. Figure 5.3 shows the results for the number of actuators varying from 1 to 25. As  $n$  increases, the resonance frequency and the damping ratio increase almost linearly as well. This result is consistent with the frequency response plots given previously in section 4.

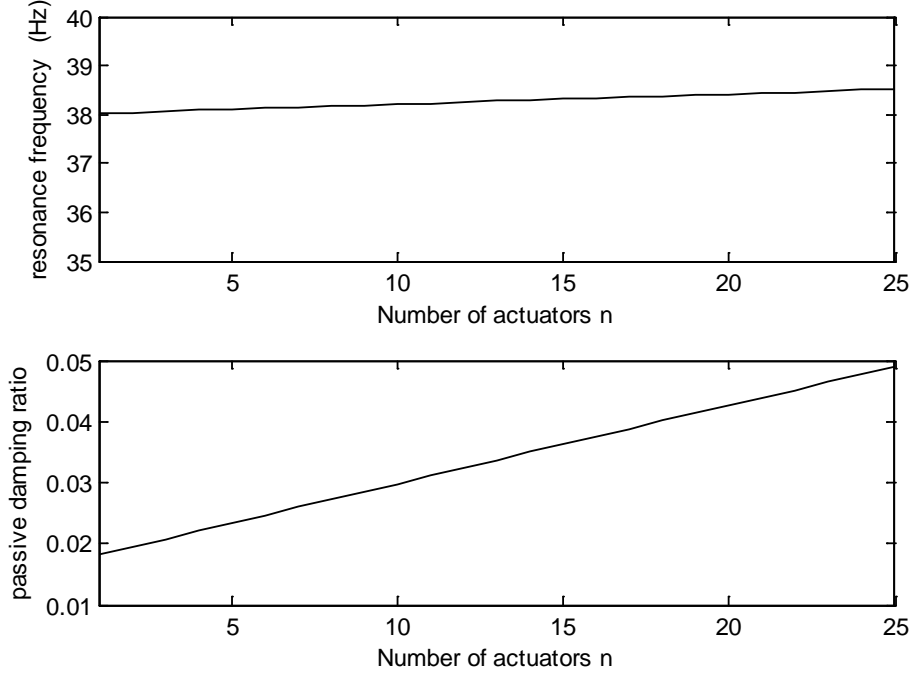


Fig. 5.3 Predicted variation of resonance frequency and passive damping ratio of the equivalent plate system from Eqs. (47) and (48).

If the coupled system is approximated as an equivalent system with modified stiffness and damping given by Eqs. (47) and (48), then the new gain for a 6dB gain margin is given by

$$g_{n6dB} = \frac{\xi_a m_e \omega_m^2}{n \omega_a} = \frac{c_a (k_m + n k_a)}{2 n k_a} \quad (49)$$

Figure 5.4 shows a comparison of the simulated gain from the Nyquist plots and those predicted by Eqs. (44) and (49) above. It is clear that the predicted gains from both Eqs.(44) and (49) predict the simulated gain from the Nyquist plots with good accuracy. The gains predicted can barely be distinguished for the example of the well damped actuators as shown in Fig. 5.4. This figure is consistent with the results obtained in [4] showing a reduced gain for an increasing number of actuators.

The new expression for maximum attenuation with the parameters given in Eqs. (47) and (48) is then given by



$$Attn (dB) = -20 \log_{10} \left( \frac{2\xi_m \omega_a}{2\xi_m \omega_a + \xi_a \omega_m} \right) = -20 \log_{10} \left( \frac{2k_a (c_m + nc_a)}{2k_a (c_m + nc_a) + c_a (k_m + nk_a)} \right) \quad (50)$$

This expression can be plotted against the number of actuators and compared to the attenuation in Fig. 5.1 as shown in Fig. 5.5. Also shown is the constant attenuation which results if Eq. (45) is used without the modified parameters given by Eqs. (47) and (48).

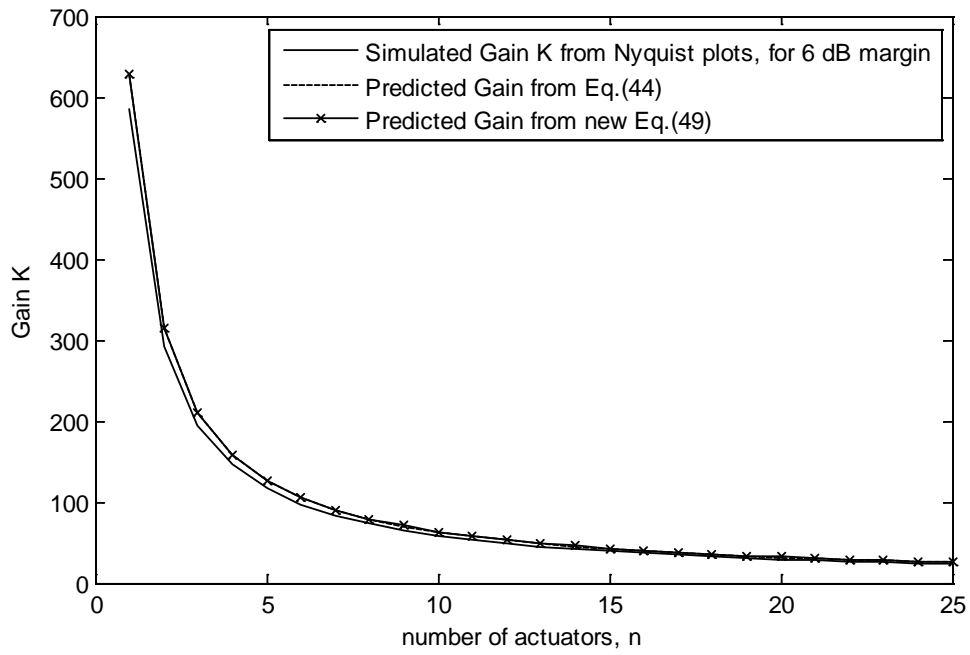


Fig. 5.4 Comparison of simulated (from Nyquist plots) and predicted gains from Eq.(44) and Eq.(49) for a 6 dB gain margin.

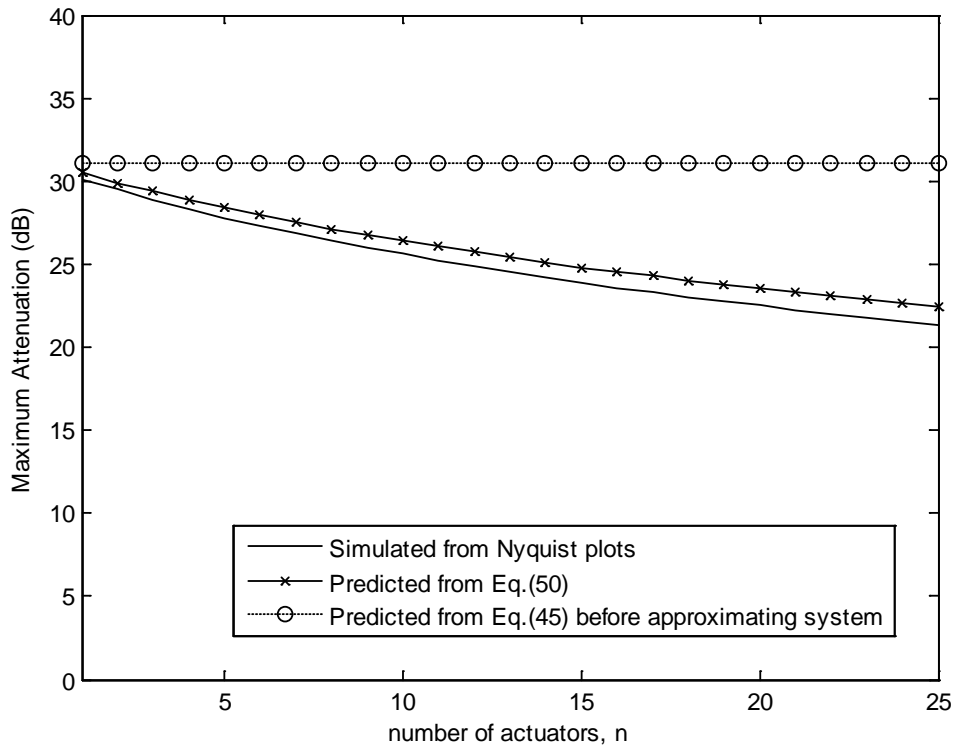


Fig. 5.5 Vibration attenuation for a 6 dB gain margin using the equivalent plate analysis of Fig. 5.2. The solid line shows the attenuation achieved in the simulations using the Nyquist plots as shown in Fig. 5.1.

Figure 5.5 shows the predicted attenuation for  $n = 1$  to 25 from Eq. (50) compared to that from the Nyquist simulations. The prediction tends to overestimate the simulated attenuation but is relatively accurate. One source of discrepancy is the way in which the feedback gains are obtained in both cases. In the simulated case, they are obtained directly from the frequency response calculations whereas in the second instance it is approximated by Eq. (50). The assumptions made in deriving Eqs.(45) and (50) are that the equipment and actuators are decoupled such that  $M_{ee}Z_{aa} \ll 1$  when  $\omega_a \ll \omega_m$ . In the example used here for the plate the ratio  $\omega_a/\omega_m \approx 0.28$ . If this ratio was much smaller it is expected that the predicted and simulated attenuations would be much closer. In the next section a study of the performance of the control of the first plate mode with several inertial actuators is presented in terms of the total kinetic energy of the plate.

## 6. PERFORMANCE OF CONTROL SYSTEM

Once the feedback gain to achieve a 6 dB gain margin is obtained as given in Eq. (49) the performance of the control system as described in section 4 can be studied. In particular, the relative change in total kinetic energy of the first plate mode can be investigated from the mobility given by Eq. (41). In this section the effects of passive attenuation of the actuators only ( $n \neq 0, g = 0$ ), that of the control system alone ( $n \neq 0, g$  given by eq. (49)) and finally that of the combined effect of the actuators and control on the plate total kinetic energy is presented (i.e. control performance compared to plate without actuators when  $n = 0, g = 0$ ). The ratio of the total kinetic energies of the plate in decibels gives an indication of the change in kinetic energy due to one cause. For example, when the plate does not have any actuators attached,  $n = 0$  and  $g = 0$  and the mobility of the plate given by Eq. (41) reduces to

$$\frac{v_{ena}}{f_p} = \frac{1}{[Z_m + j\omega m_e]} \quad (51)$$

When actuators are attached and no control on, the mobility is given by

$$\frac{v_{enc}}{f_p} = \frac{1}{[nZ_a + Z_m + j\omega m_e] - n \left[ \frac{Z_a^2}{(Z_a + j\omega m_a)} \right]} \quad (52)$$

Hence it is possible to calculate the ratio of the total kinetic energy of the plate per unit primary force with and without actuators and this gives an indication of the change in total kinetic energy due to the addition of the actuators. Similarly the effect of control can be studied compared to the case of the plate without and with actuators. Figure 5.6 summarises the three cases mentioned above. The addition of the actuators to the plate introduces passive damping to the plate and hence reduces the plate vibration. As the number of actuators increases the passive reduction increases. On the other hand, the effect of control using multiple actuators has an opposite effect on the attenuation. Initially a large attenuation is obtained with a single actuator which then decreases as the number of actuators increases. This result is consistent with the peak attenuation result obtained in Fig. 5.5. The combined attenuation due to the passive and active effects however shows that there is a net increasing reduction (albeit small) in the total kinetic energy of the plate as the number of actuators increases. This result is also consistent with the results obtained in [4] with the exception of the change in kinetic energy due to control for a small number of

actuators. In the previous study the attenuation due to a single actuator is small and increases to a maximum before decreasing again as the number of actuators increases. The difference is mainly due to the fact that the previous study included up to 53 plate modes whereas a single plate mode is considered in the example given here.

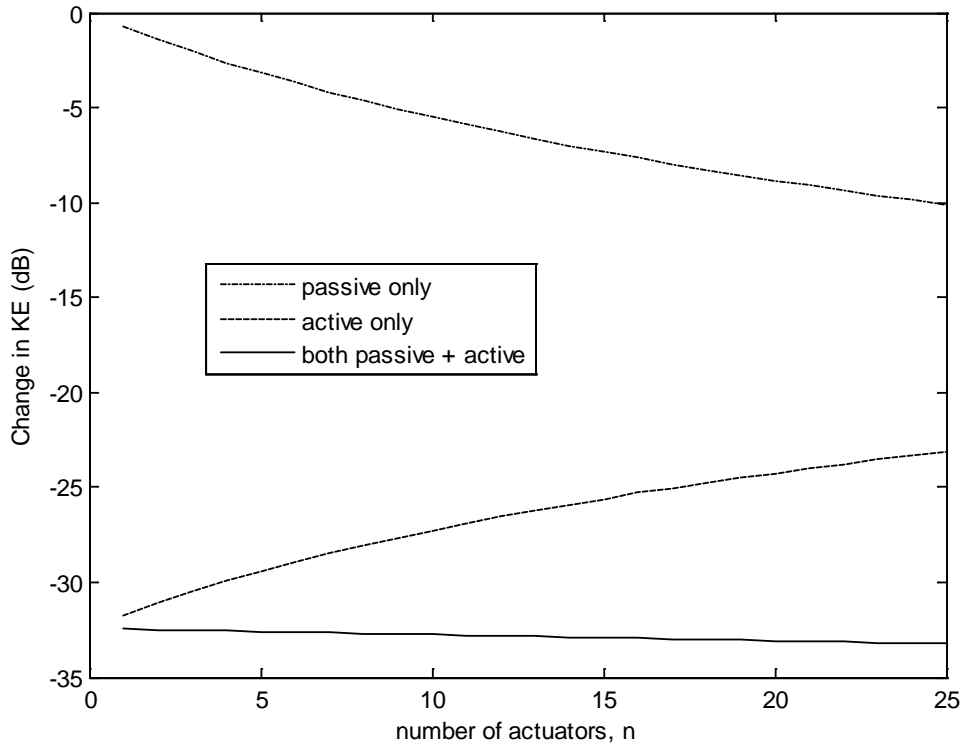


Fig. 5.6 Change in the total kinetic energy of the first plate mode due to passive control, active control and combined passive and active control.

## 6. SUMMARY

In this report the feedback active isolation problem using an inertial actuator is extended from the single-channel to the multiple channel case. In the first instance an example of a two-actuator system is considered and the equation for the frequency response derived. The result shows that the response per unit actuator input is dependent on the number of actuators as well as the total mechanical input impedance of the coupled system. The magnitude of the frequency response tends to increase almost proportionally with the number of actuators when the number of actuators is small. In this case the response is almost doubled in magnitude. If the number of actuators is more than 2, the response changes in a more significant way via the sum of the mechanical impedance of all the actuators. If the equipment/plate and actuators are such that  $\omega_a \ll \omega_m$  they can be assumed decoupled and the magnitude of the open-loop frequency response is mainly proportional to the number of actuators.

The system response consists of two resonance peaks with the first one related directly to the actuator resonance. This resonance frequency changes only slightly with an increasing number of actuators. However, its magnitude increases almost proportionally. The second resonance is that due to the complete coupled system mainly associated with the equipment/plate resonance. As more actuators are added the corresponding resonance frequency increases indicating a stiffer system. At the same time the damping of this frequency also increases. The net effect of the addition of more actuators on the system response can be understood from the Nyquist plots. The left-hand loop which determines stability tends to expand faster than the right-hand loop which determines the peak vibration attenuation. Therefore, increasing the number of actuators requires a reduction in feedback gain for a given stability margin but at the same time a reduced peak vibration attenuation results.

An example application consisting of the first mode of a plate as the equipment with multiple inertial actuators was investigated. Simulation from the frequency response calculations shows that the peak attenuation that can be achieved with more actuators tends to decrease. An approximate representation of the coupled system by an equivalent single-degree-of-freedom system shows that the natural frequency and damping of the system increase with more control channels. This also indicates that the multi-channel system behaves as a stiffer and more damped system. An expression for the peak vibration reduction could be approximated from the decoupled system equation with modified parameters. The predicted results are in good agreement with the simulated results from the Nyquist plots provided that the actuators-plate can be assumed decoupled for  $\omega_a \ll \omega_m$ .

Finally the performance of the simple one-degree-of-freedom system revealed that the total kinetic energy of the plate mode reduced after addition of the passive actuators. When control is introduced however, the kinetic energy of the plate increases as the number of actuators increases. Hence the performance due control alone tends to decrease. This is due to the fact that the addition of the actuators changes the open-loop frequency response of the system in such a way that to maintain a given stability margin the feedback gain has to be reduced. This has been verified by the Nyquist plots of the system as well as from the gain equations. The combined

passive/active control performance shows that the kinetic energy of the plate mode decreases as the number of actuators increases.

The example used in this report is limited due to the fact that a single plate mode was considered. Although the results are consistent with the previous study given in [4] where a plate including 53 modes is used, there are some differences with regards to the control results. A future study can use the general model developed in this report with the mobility of the base equivalent to that of the plate in [4]. The equipment and mount parameters can be replaced by those of the vibration sensor casing mass and its dynamic parameters. In practice for a securely fixed casing the casing stiffness and damping can be assumed very large such that the casing acts as if it is attached directly to the plate. For this more realistic system, the generalized open-loop frequency response is still given by Eq.(34) but with  $M_{ee}$  given in Eq.(6) modified to

$$M_{ee} = \frac{M_e}{1 + M_e/M_b}$$

for the impedance of the casing  $Z_m \rightarrow \infty$ . Here  $M_b$  is the mobility of the plate. Using this model with a given plate mobility it will be possible to study the system performance by simulation as described in this report for any number of plate modes. A more direct comparison with the results in [4] can then be obtained and conclusions drawn.

## 7. REFERENCES

- [1] S. J. Elliott, M. Serrand and P. Gardonio, "Feedback stability limits for active isolation systems with reactive and inertial actuators," ASME Journal of Vibration and Acoustics, **123**, 250-261, (2001).
- [2] S. J. Elliott, P. Gardonio and B. Rafaely, "Performance evaluation of a feedback active isolation system with inertial actuators," ISVR Technical Memorandum No. 832, (1998).
- [3] G. F. Franklin, J. D. Powell and A. Emani-Naeini, "Feedback control of dynamic systems, third edition, 1994, Addison Wesley, Reading, MA.
- [4] O. N. Baumann and S. J. Elliott, "The stability of decentralized multichannel velocity feedback controllers using inertial actuators," The Journal of The Acoustical Society of America, **121** (1), 188-196, (2007).